ГОРИЗОНТЫ РАДИОАСТРОНОМИИ

Парийский Ю.Н.
САО

22 сентября 2008г

ПЛАН

- Особенность 21 века
- Наука и Радиоастрономия
- Радиотелескопы

Физика и Астрономия

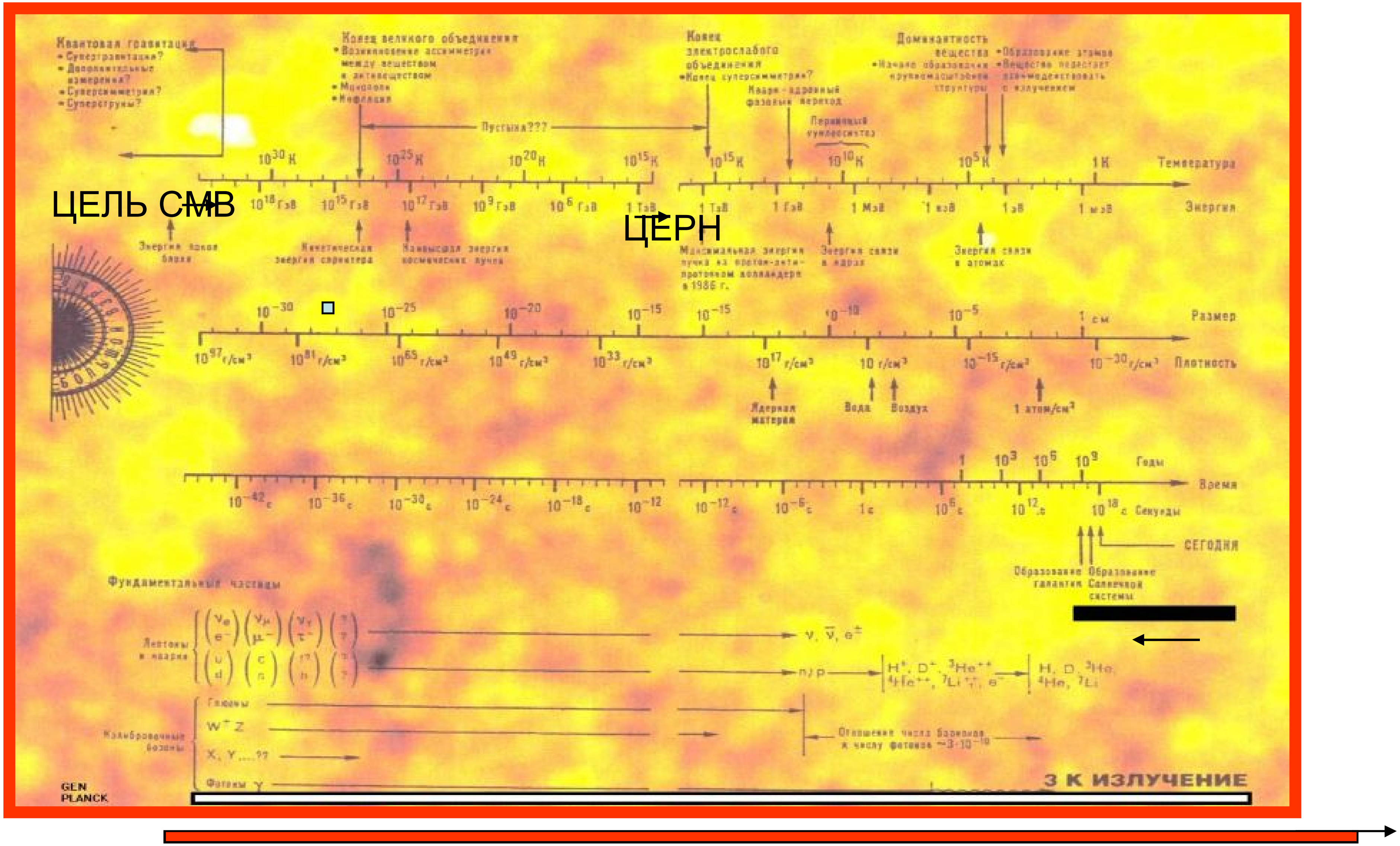

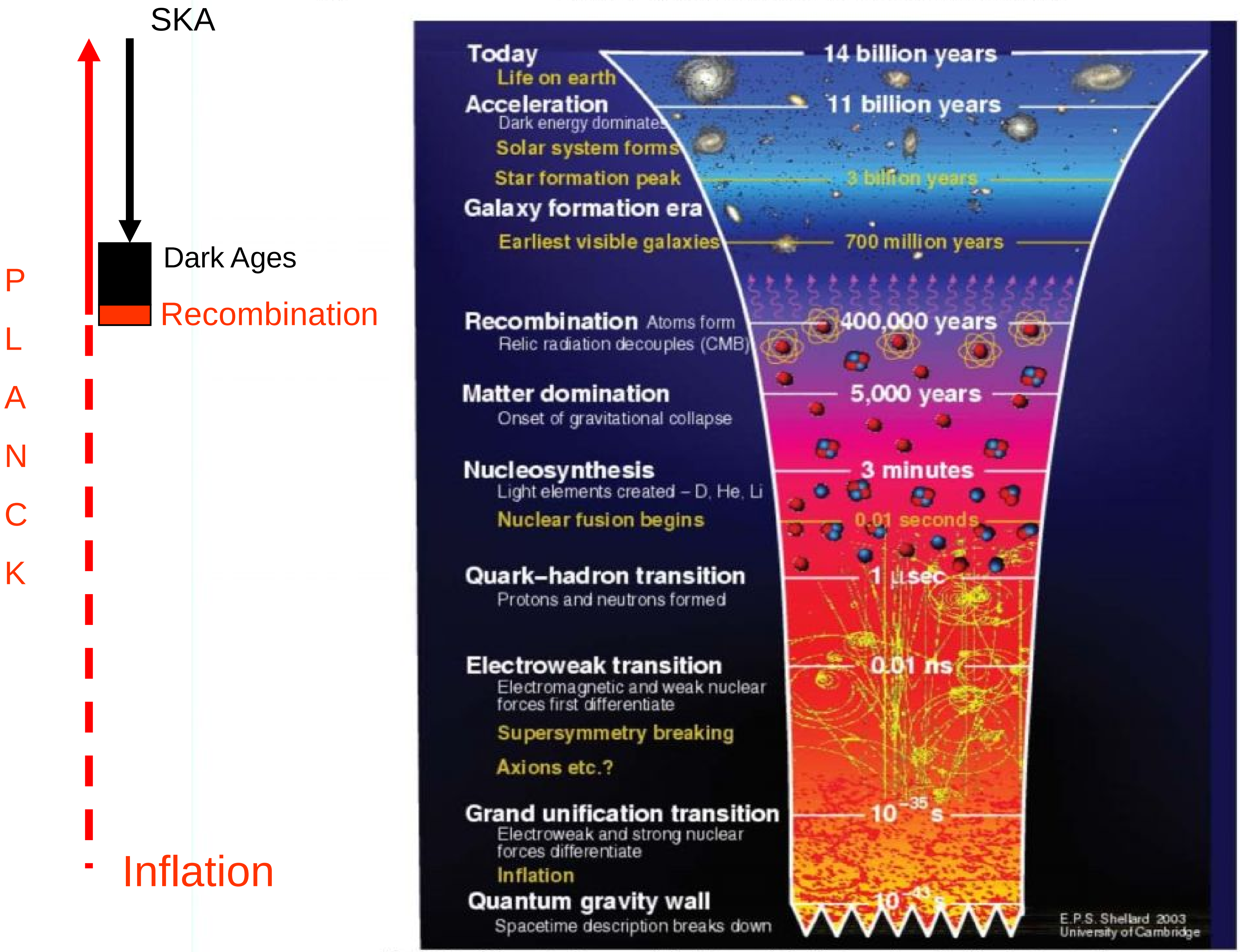

FIG 2.20.—Schematic diagram of the history of the Universe from the Planck time to the present.

РТ и ЦЕЛИ

- Объекты

- Протообъекты

РАЗНЫЕ РЕШЕНИЯ!

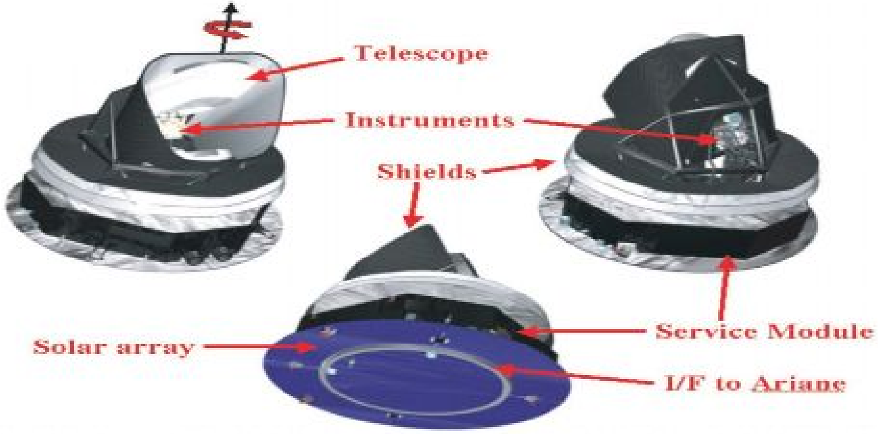

FIG 1.1.— Main elements of *Planck*. The instrument focal plane unit (barely visible) contains both LFI and HFI detectors. The function of the large baffle surrounding the telescope is to control the far sidelobe level of the radiation pattern as seen from the detectors. The specular conical shields (often called "V-grooves") thermally decouple the Service Module (which contains all warm elements of the satellite) from the Payload Module. The satellite spins around the indicated axis, such that the solar array is always exposed to the Sun, and shields the payload from solar radiation. Figures courtesy of Alcatel Space (Cannes).

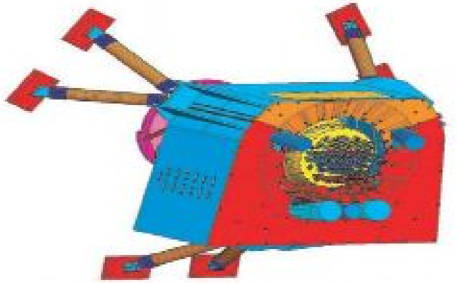

FIG 1.2.—*Planck* focal plane unit. The HFI is inserted into the ring formed by the LFI horns, and includes thermal stages at 18 K, 4 K, 2 K and 0.1 K. The cold LFI unit (20 K) is attached by bipods to the telescope structure.

provides highly efficient radiative coupling to cold space, and a high degree of thermal isolation between the warm spacecraft bus and the cold telescope, baffle, and instruments. The cooling provided by the passive system leads to a temperature of ~ 50 K for the telescope and baffle. The active cryocoolers further reduce the temperature to 20 K and 0.1 K for the instruments.

Самый глубокий CMB поляризационный эксперимент

QUIET Characteristics

Component	ν_{center} [GHz]	FWHM [']	FOV [°]	N_{feeds} Pol	N_{feeds} Temp	T^a_{sys} [K]	$\Delta\nu$ [GHz]	Q+U Sensitivity[b] Per Feed [$\mu K\, s^{1/2}$]	Q+U Sensitivity[b] Array [$\mu K\, s^{1/2}$]
QUIET Phase I									
1 m	40	41	11	17	2	27	8	159	39
1 m	90	18	12	83	8	54	18	248	27
QUIET Phase II									
2 m	40	23	13	166	16	27	8	159	12
7 m	40	9	6	83	8	27	8	159	17
2 m	90	10	12	714	80	54	18	248	9
7 m	90	3.8	5	357	40	54	18	248	13

[a] Antenna temperature units, based on field-tested MMIC amplifier noise + 2.73 K + NRAO model atmosphere at 45° elevation.

[b] Thermodynamic units, including both Q and U from correlation polarimeter, with normalization $Q = (T_x + T_y)/2$

QUIET II has 3–4 times better polarization sensitivity than Planck at 100 GHz!

Cryostat—91-element Phase I

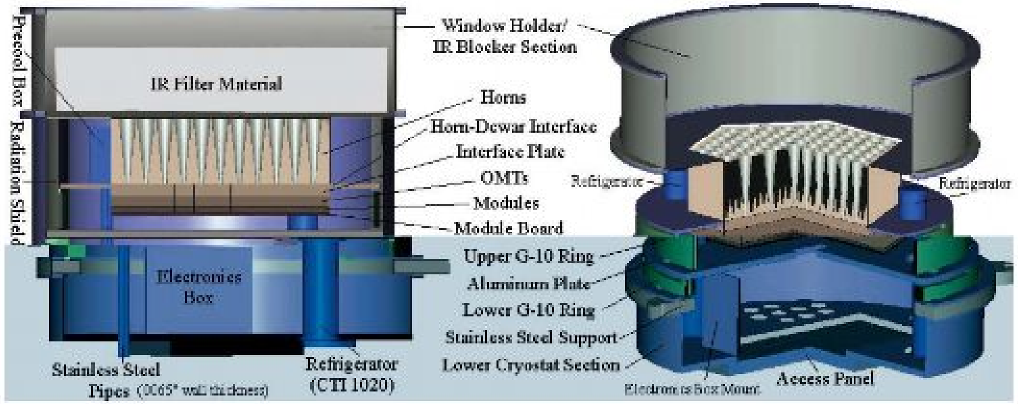

Modules

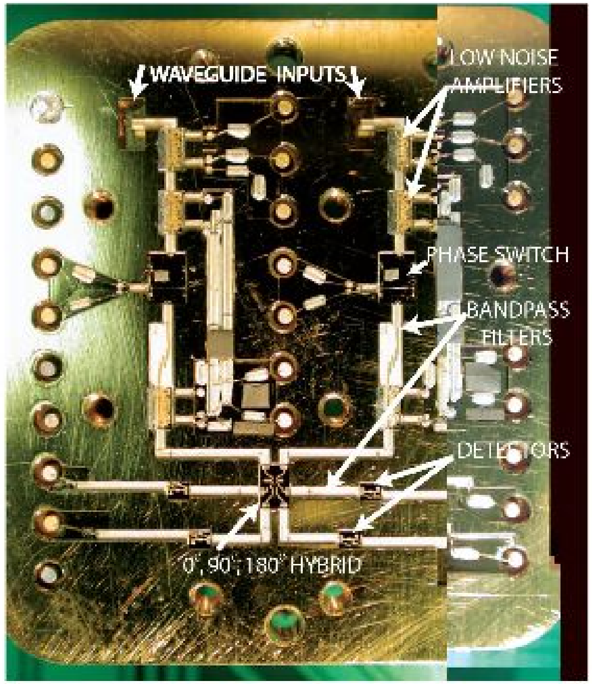

W-band, 1.25″ × 1″

W-band

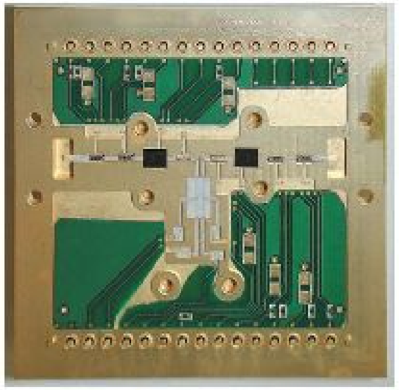

Q-band, 2″ × 2″

mm и Россия

- Доклады АКЦ (Д70, МИЛЛИМЕТРОН)
- Отдельное обсуждение по действующим РТ

b.

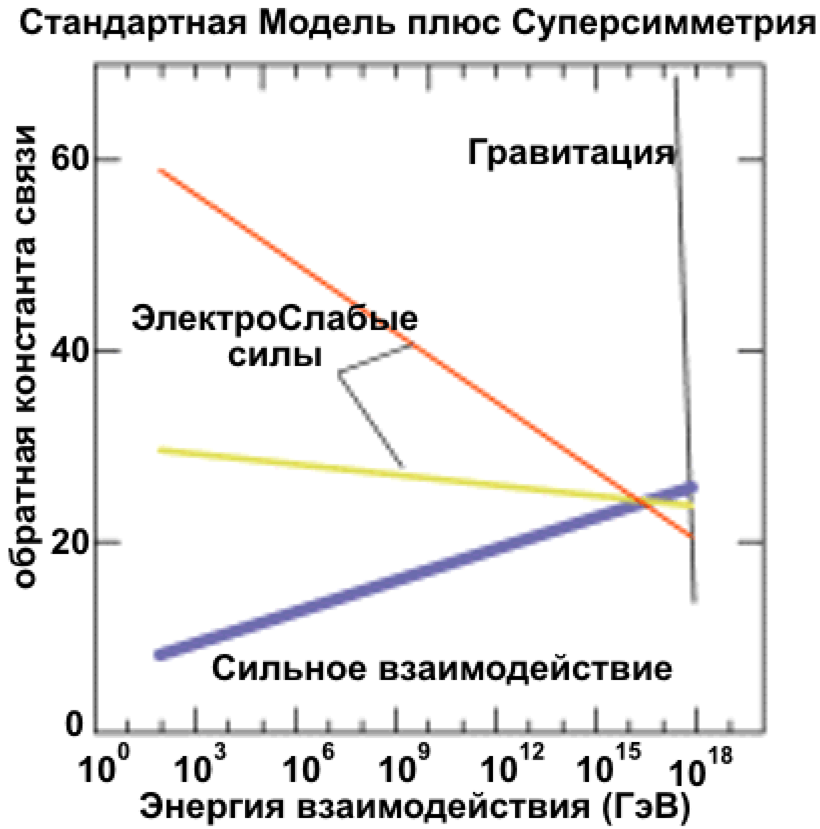

Стандартная Модель плюс Суперсимметрия
обратная константа связи
0
20
40
60
Гравитация
ЭлектроСлабые
силы
Сильное взаимодействие
10^0
10^3
10^6
10^9
10^12
10^15
10^18
Энергия взаимодействия (ГэВ)

Самый крупный наземный проект 21 века в основном диапазоне

Square Kilometre Array

SKA

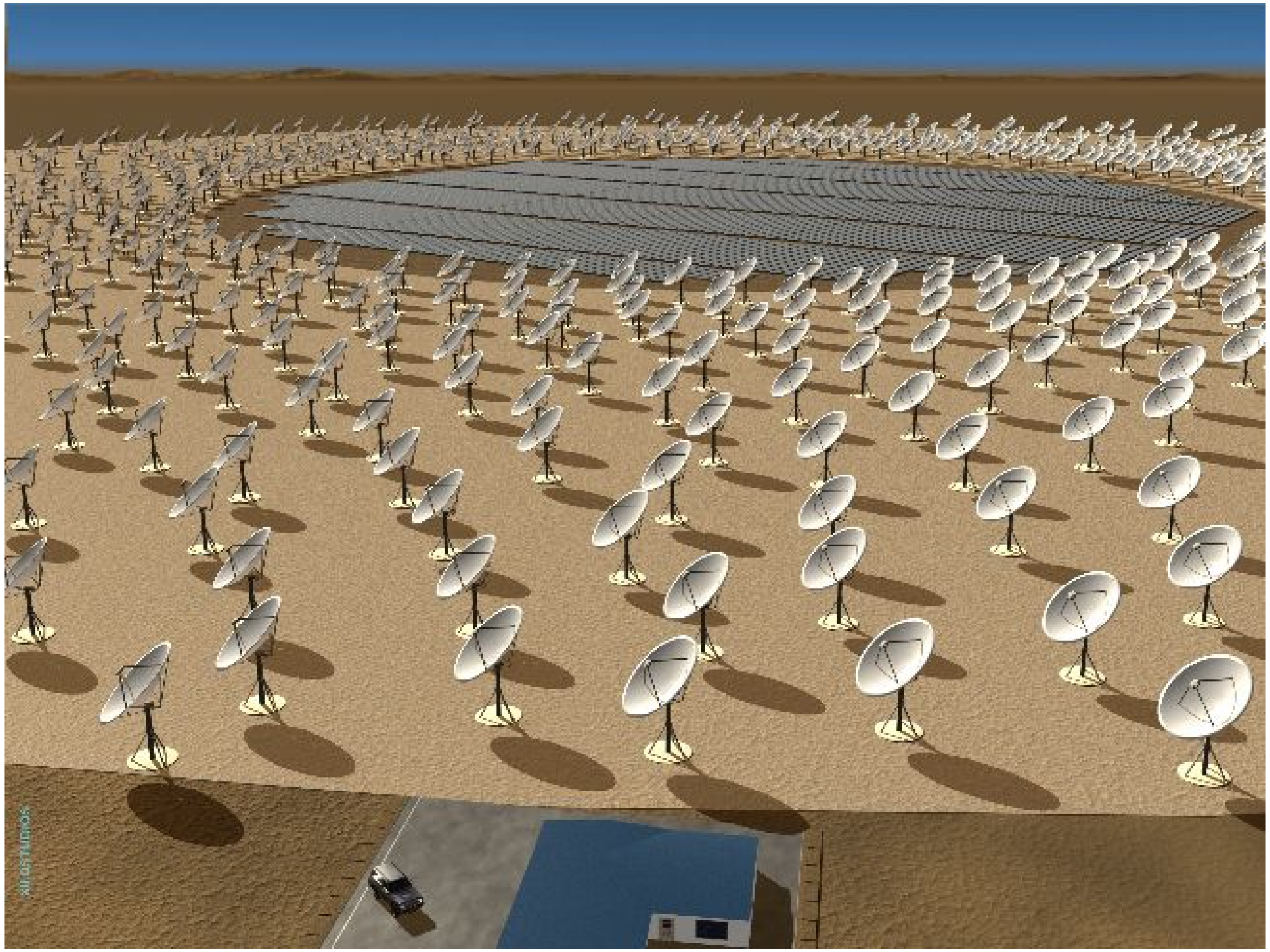

SKA Timeline

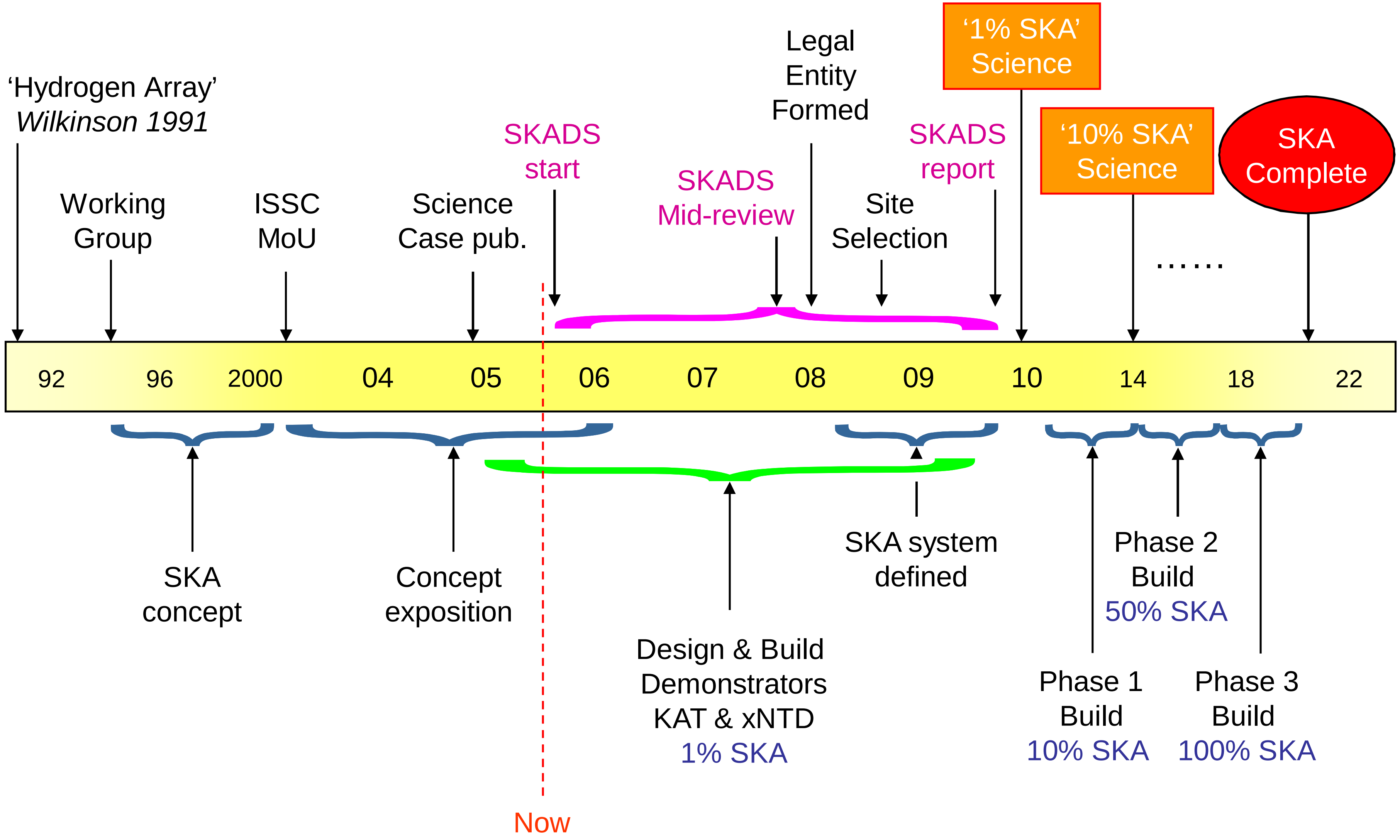

От mJy к nanoJy
>50% неба покрыто радиоисточниками…

7

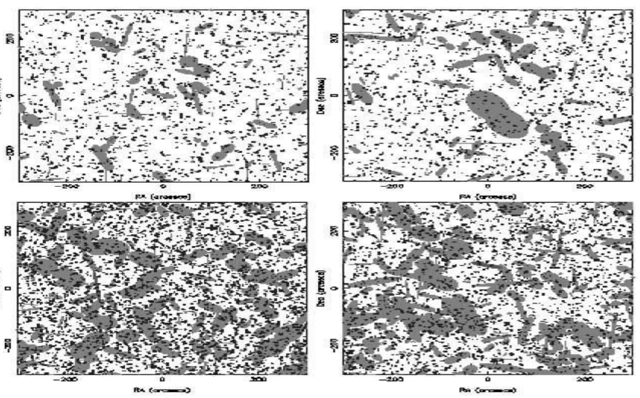

Figure 2. Simulated sky images at 1.4 GHz, showing a 10 arcmin square region for flux density limits of 1 μJy (upper) and 100 nJy (lower). The difference between the pair of images at the same flux density illustrates cosmic variance, with nearby large-lobed sources dominating the right-hand plots. There are 5 populations of sources shown: FRI galaxies (light, double-lobed), FRII galaxies (dark, double-lobed), starforming galaxies (dark, single disk), beamed FRIIs (dark, star), and FRIs (light, star).

SKA и популяции PS

6

Table 1
Predicted source surface densities at 1.4 GHz.

Population	10 μJy N / deg^2	10 μJy Cover fraction	1 μJy N / deg^2	1 μJy Cover fraction	100 nJy N / deg^2	100 nJy Cover fraction
FRI	1,207	4.10^{-2}	4,028	0.136	10,162	0.340
FRII	55	3.10^{-3}	56	3.10^{-3}	56	3.10^{-3}
star-forming	7,361	2.10^{-3}	52,798	2.10^{-2}	135,806	0.05
Total	8,623	5.10^{-2}	56,822	0.162	146,024	0.394
Minimum resolution / arcsecs	0".86		0".17		0".07	
% of sources overlapped (line-of-sight)	10%		25%		60%	

Table 2
Predicted source distribution per square degree at 1.4 GHz.

Самый большой мм. проект

- **Atacama Large Mm Array**

- **64 x D14m**
- **800 GHz- 30 GHz**
- **Size (variable) 0.5km-2km**

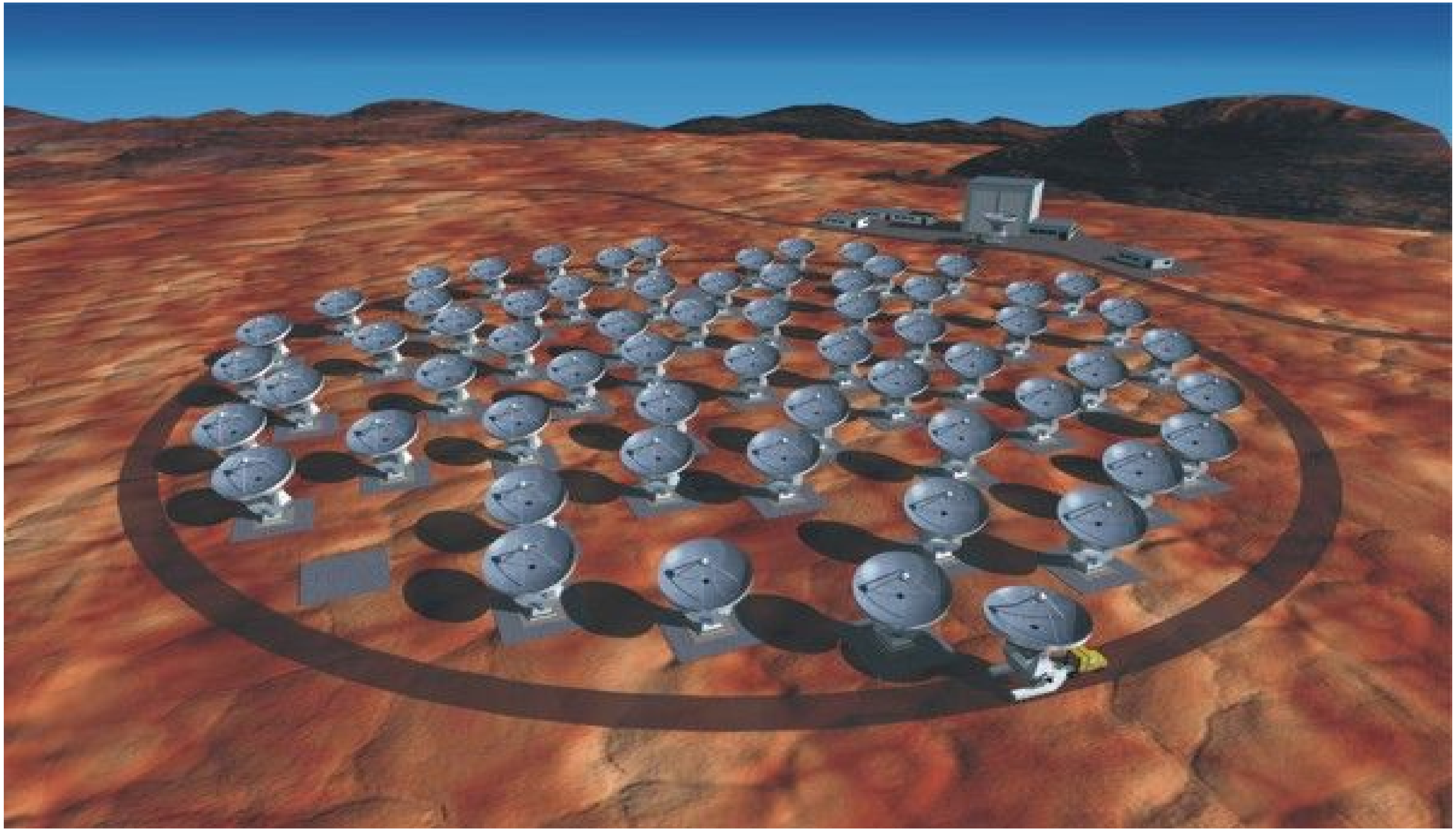

ALMA, первый спектр

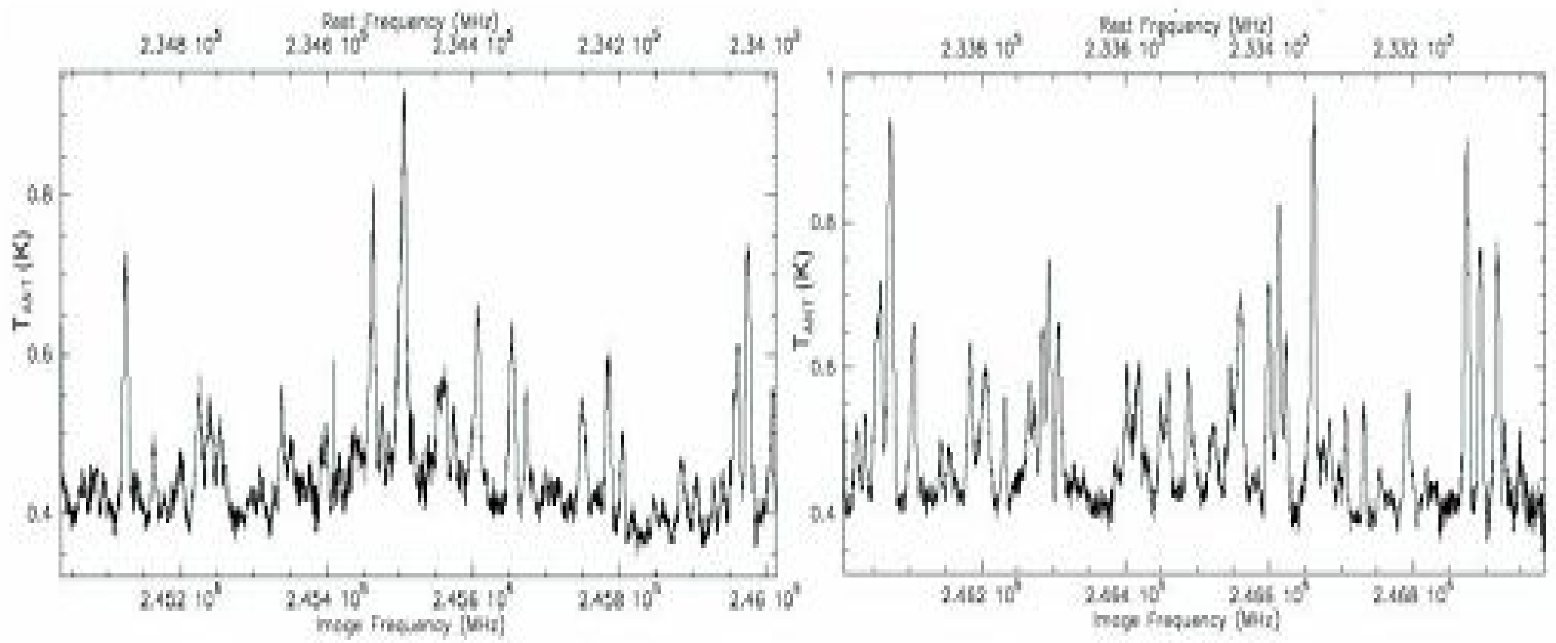

Fig. 6. Illustration of the 2 GHz wide IF bandwidth achievable using both filter banks. These data are part of one continuous 30 minute scan of the SgB2(N) region.

Фокальные фары и интеграция SKA и CMB команд?

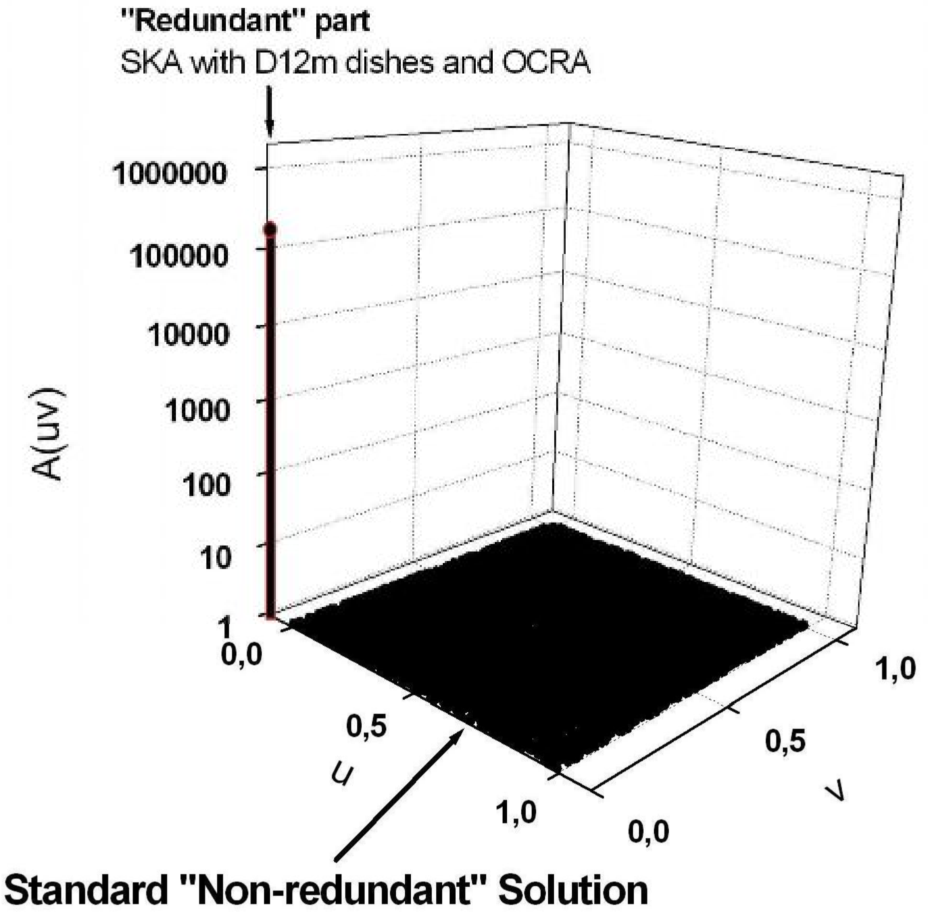

Самый крупный низкочастотный проект

- Low Frequency Array

- **LOFAR**

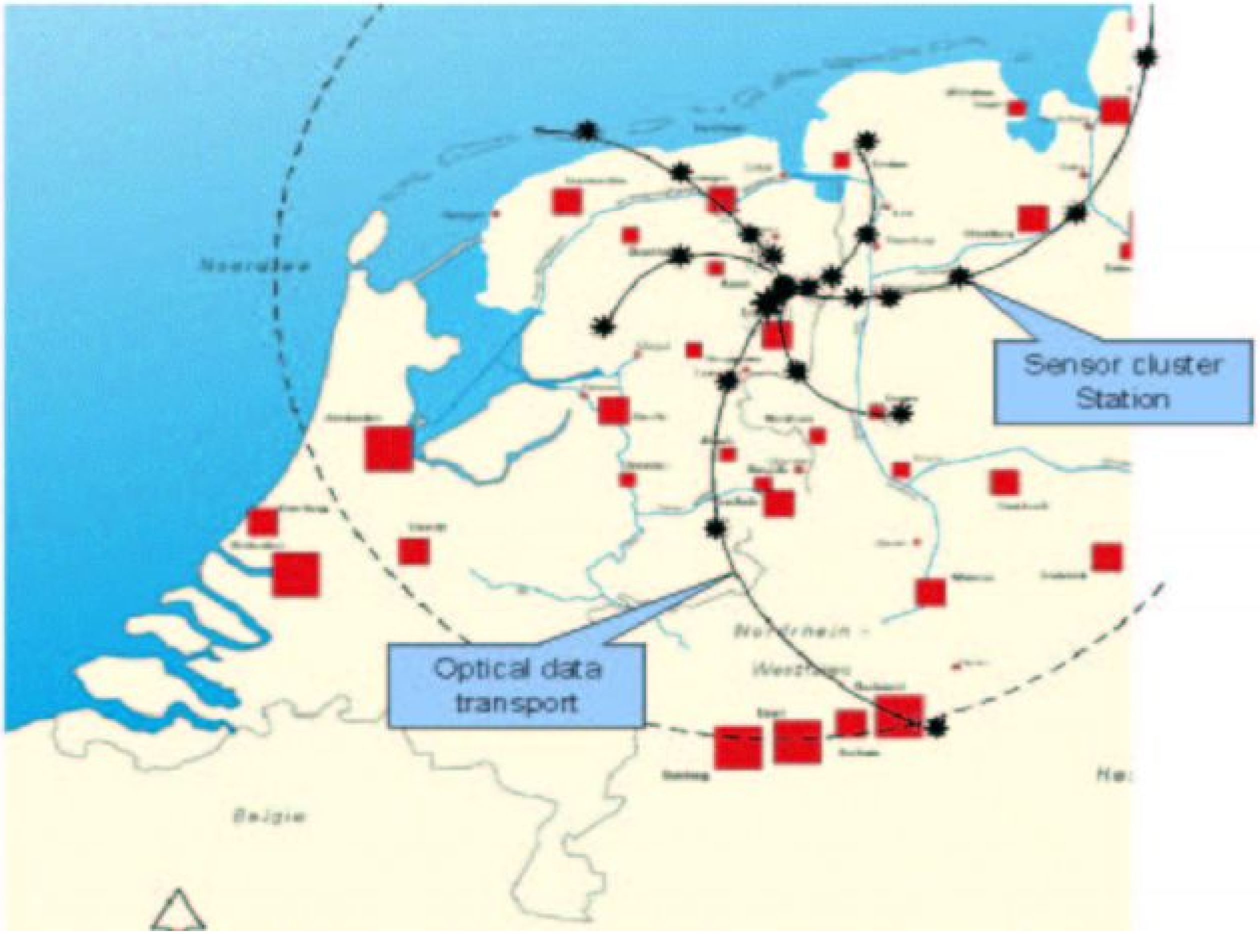
Sensor cluster
Station
Optical data
transport

Figure 1. An artist impression of the candidate layout of (a Netherlands version of) an individual LOFAR station.

Новая ФИЗИКА и 21 век

- LAMBDA (DE?)
- DM
- M-Theories ?

News: Holes in NVSS and CMB

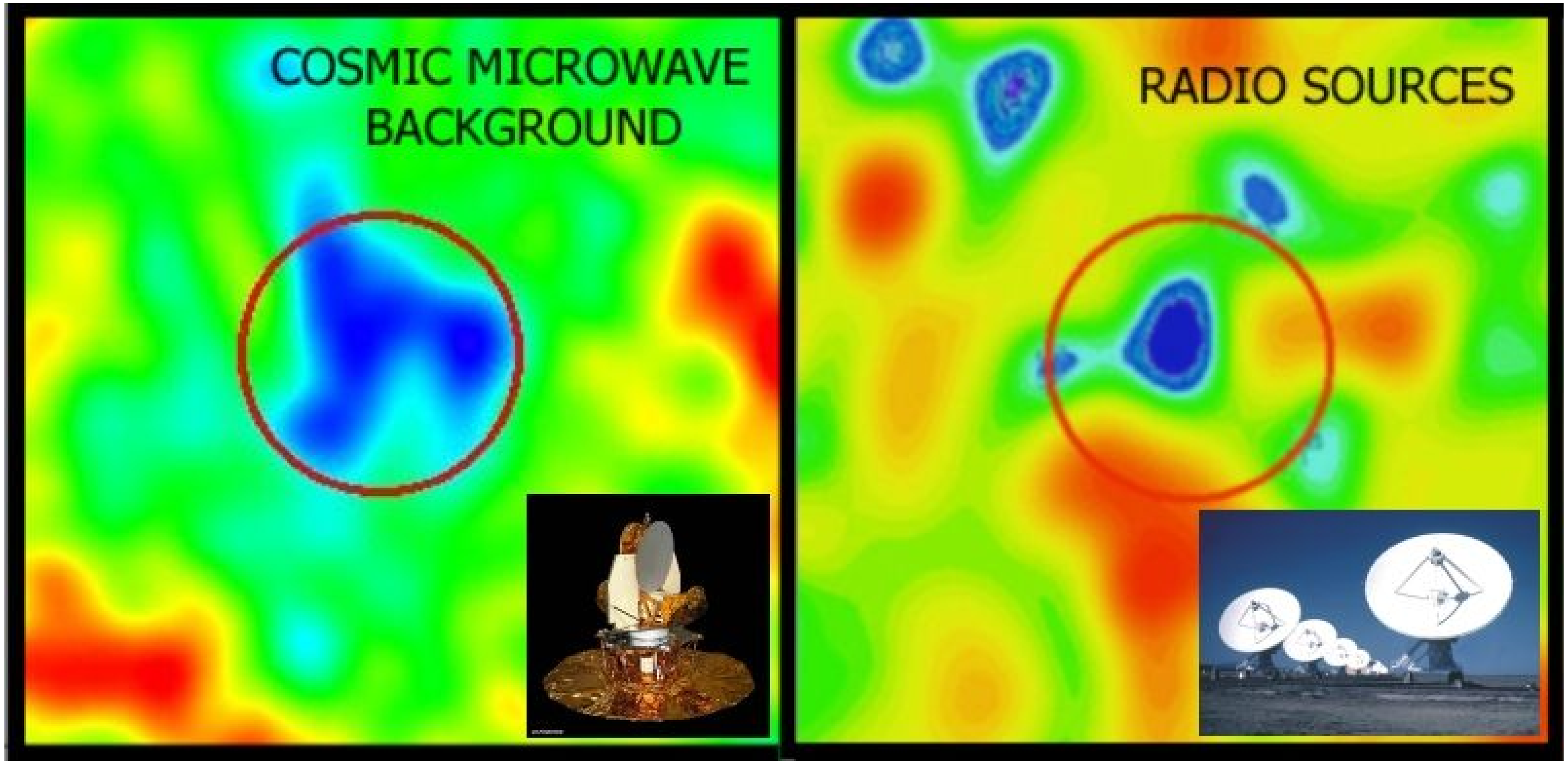

К поиску DE, DM по ISW эффекту

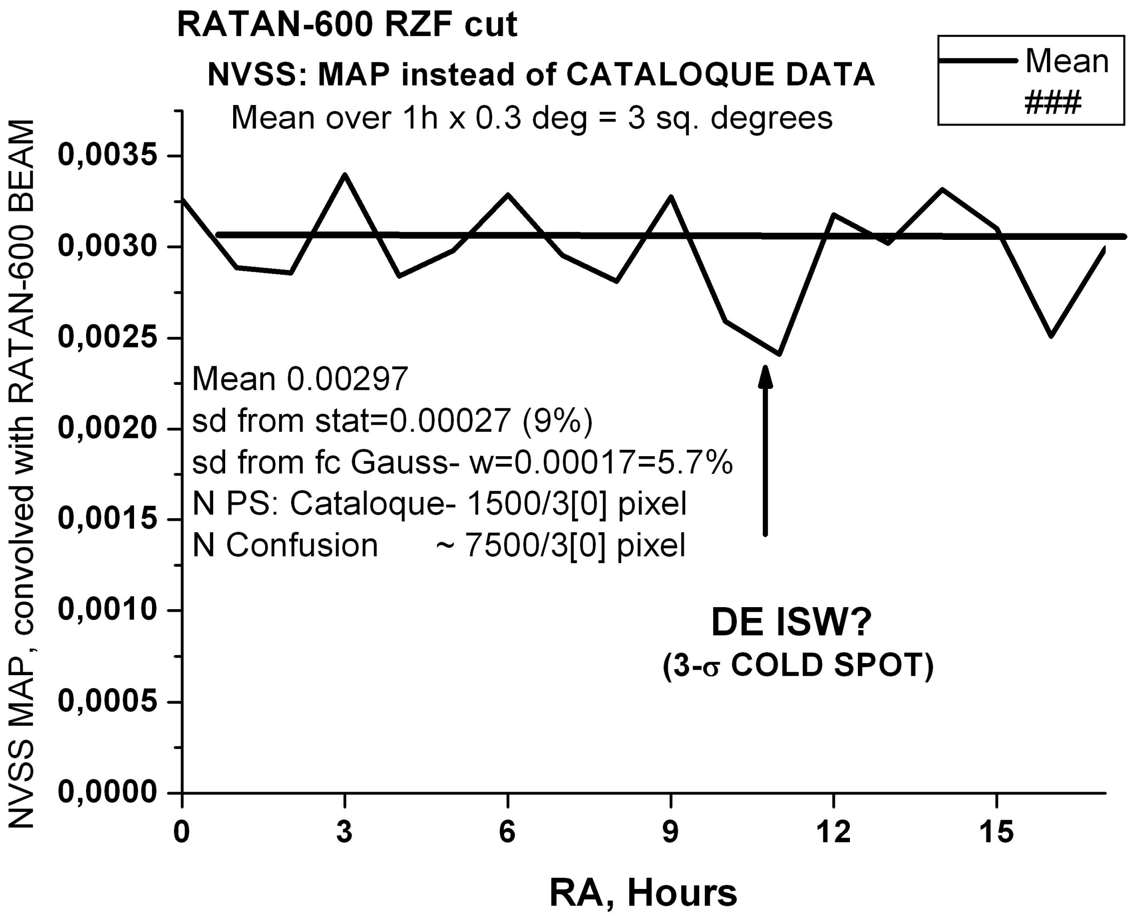

WD:ColdSpot|NNBlenaN-ColdSpot

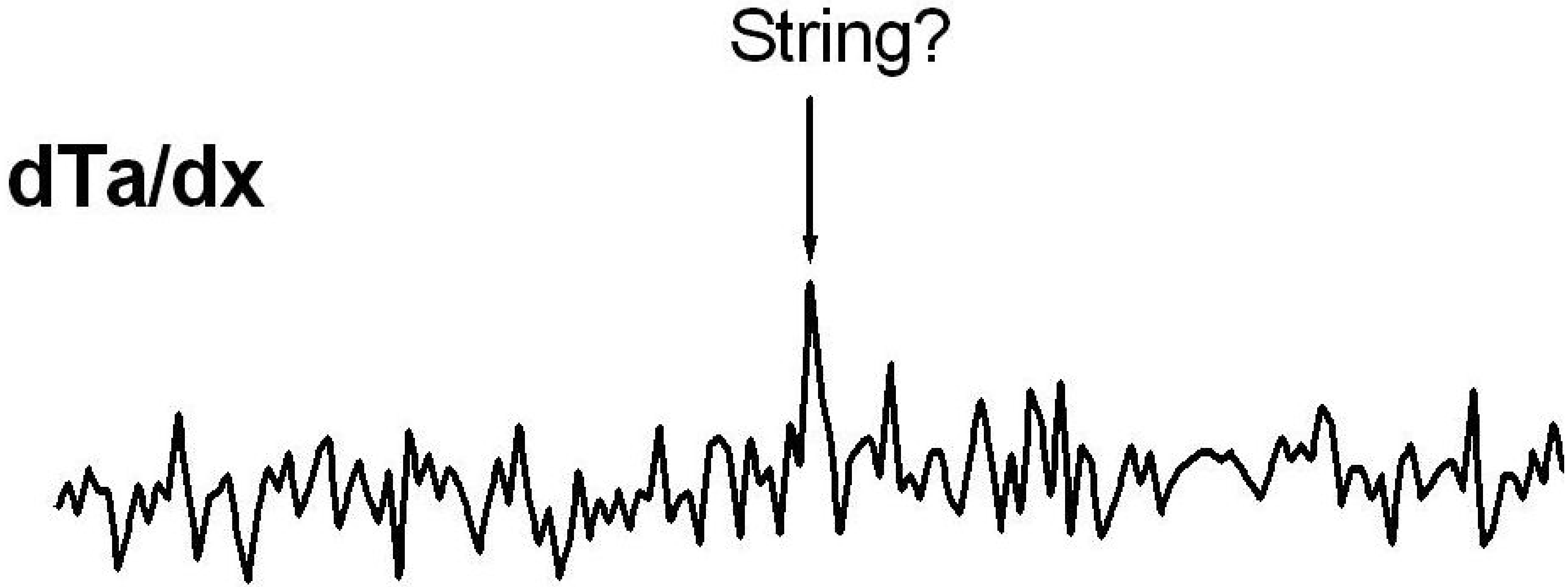

All Years and Wavelengths DATA used

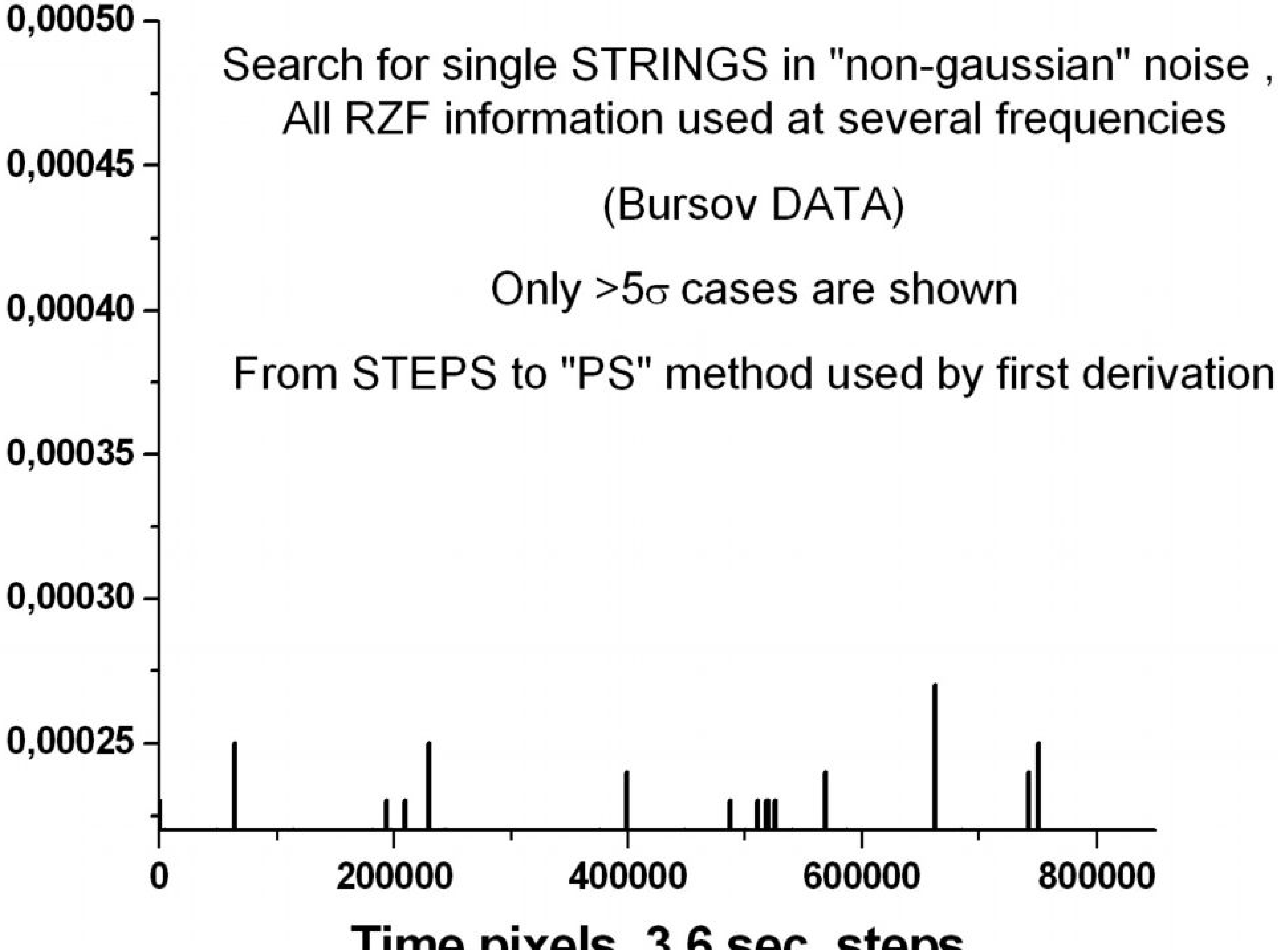

0,00050
0,00045
0,00040
0,00035
0,00030
0,00025
Search for single STRINGS in "non-gaussian" noise ,
All RZF information used at several frequencies
(Bursov DATA)
Only >5σ cases are shown
From STEPS to "PS" method used by first derivation
0
200000
400000
600000
800000
Time pixels, 3.6 sec. steps

КОНЕЦ

Цели ФИЗИКИ и КОСМОЛОГИИ

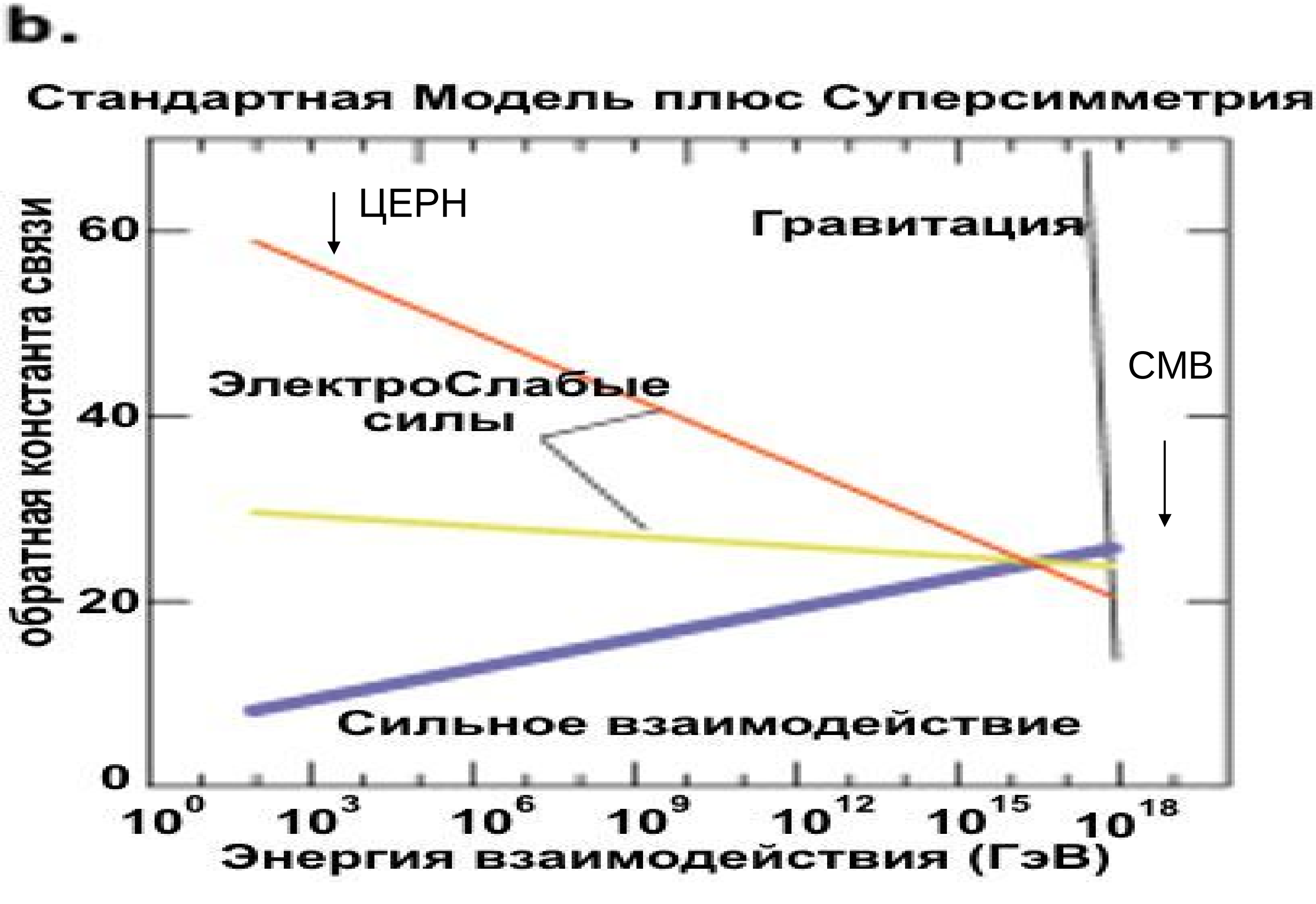

formed with the help of separate dish. Such a RH method at 8 mm wave is under exploitation now at the RATAN-600 for support of observations at 3 mm.

Fig. 1a.

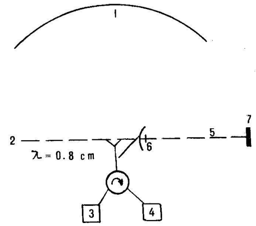

Fig. 1b.

1 - main mirror;
2 - secondary mirror's focal line;
3 - transmitter;
4 - receiver;
5 - reference signal;
6 - additional antenna;
7 - reflecting shield.

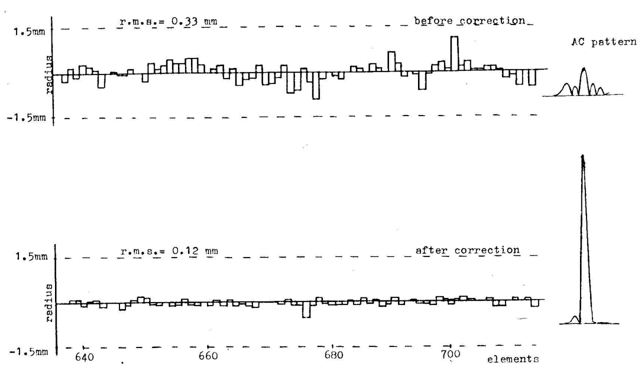

Fig.2

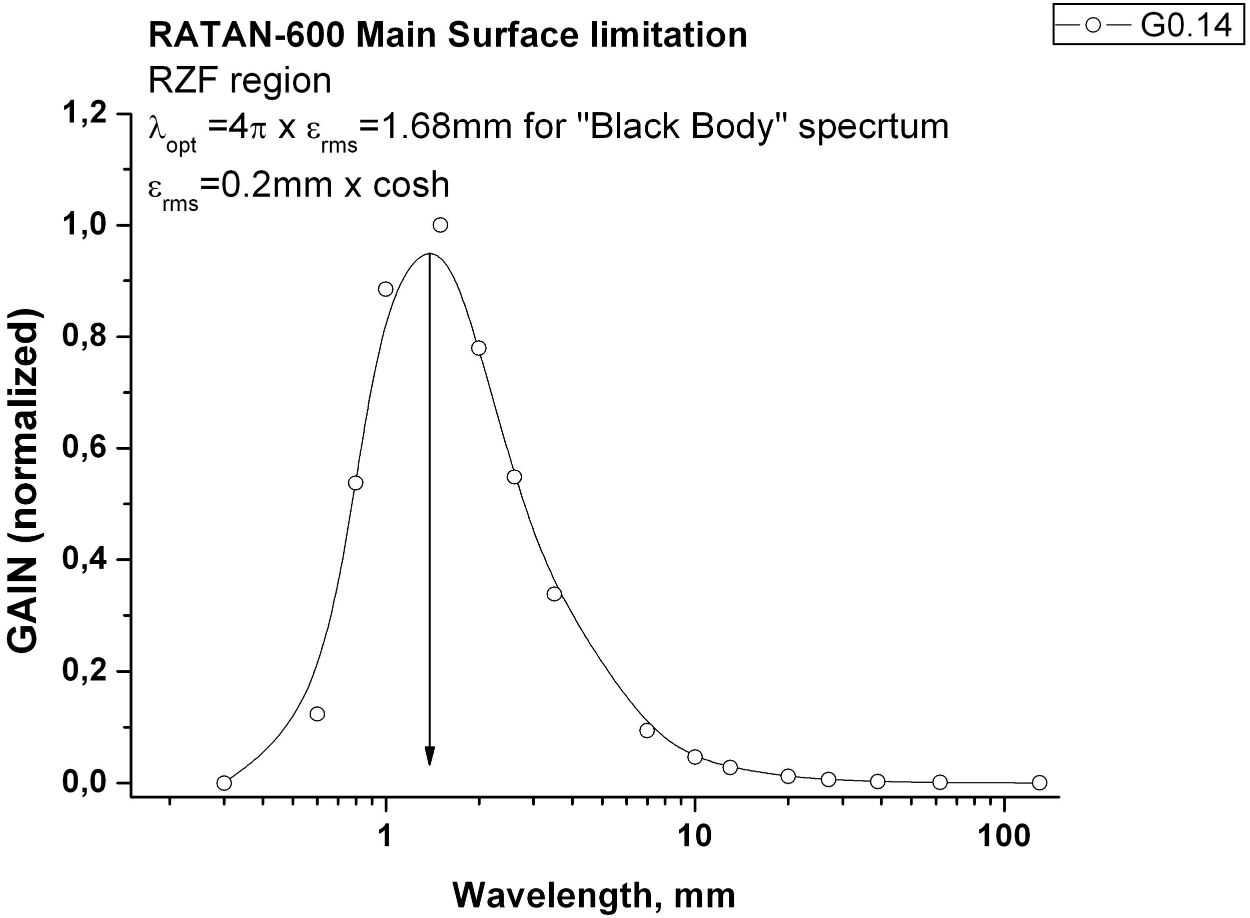

CW:|PARnew|mmALMA-Gmax

On the stability of the main surface
Inside 1 month r.m.s. difference ~0.1mm

.ity.

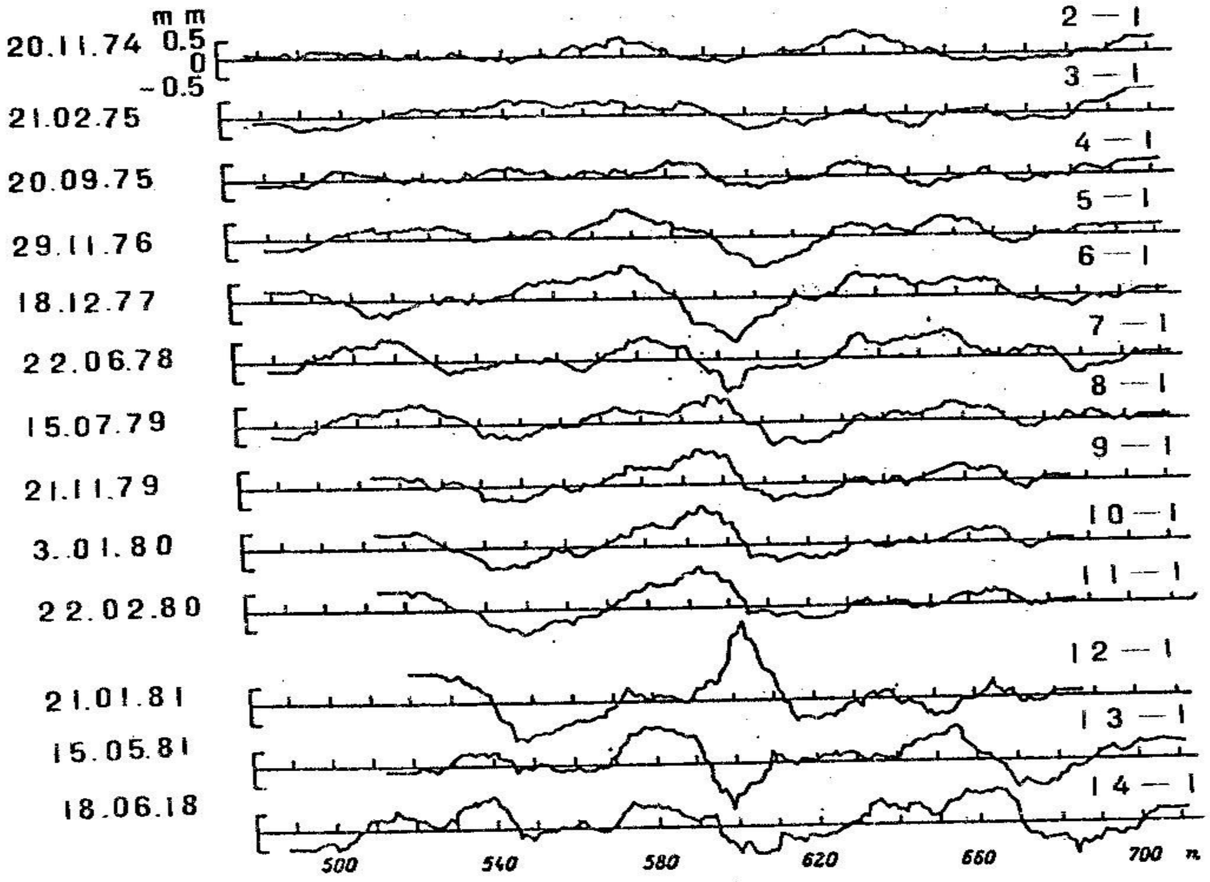

Fig. 3
Large-scale deformations of the main reflector.

On the stability of the main surface
Inside 1 month r.m.s. difference ~0.1mm

.ity.

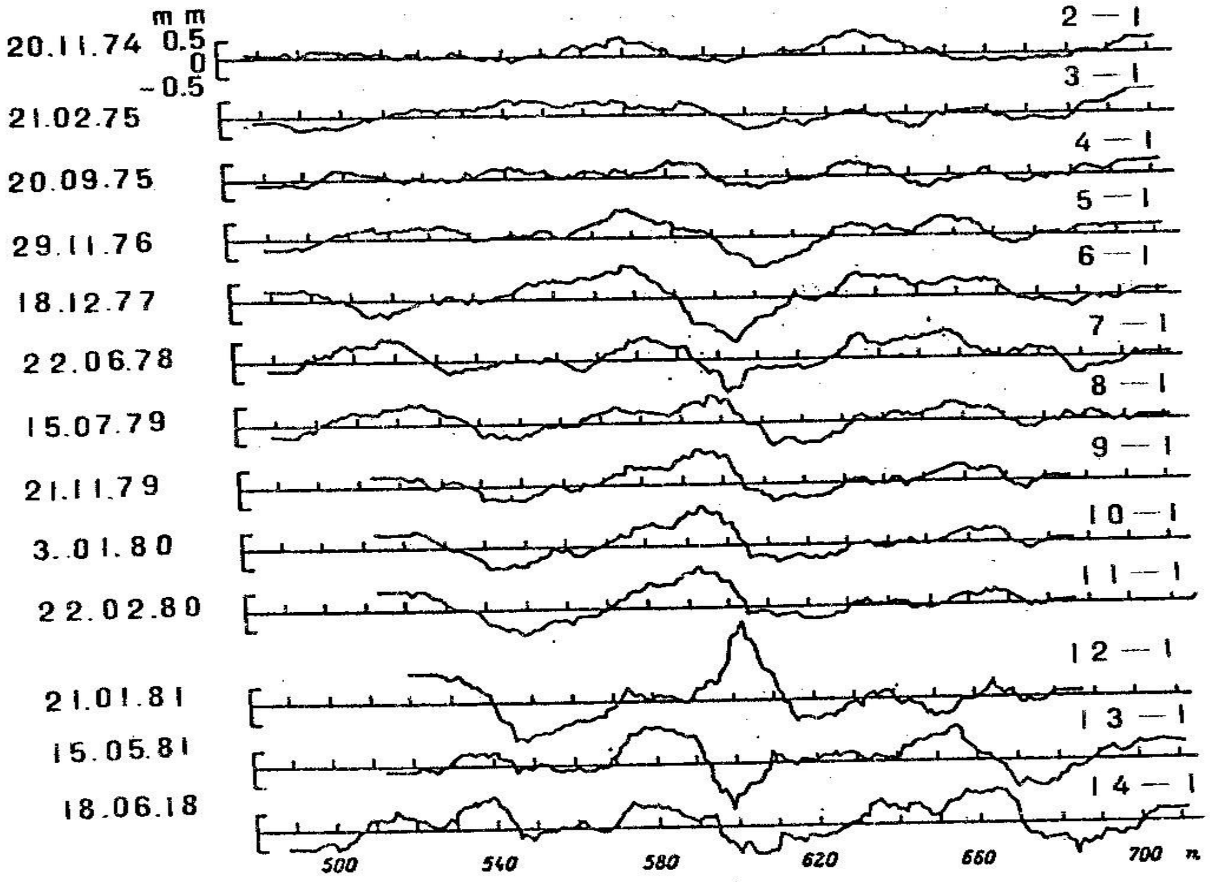

Fig. 3 Large-scale deformations of the main reflector.


03:10